PAS kinase is activated by direct SNF1-dependent phosphorylation and mediates inhibition of TORC1 through the phosphorylation and activation of Pbp1

Desiree DeMille[a], Bryan D. Badal[a], J. Brady Evans[a], Andrew D. Mathis[b], Joseph F. Anderson[a], and Julianne H. Grose[a]

[a]Department of Microbiology and Molecular Biology and [b]Department of Chemistry, Brigham Young University, Provo, UT 84602

ABSTRACT **We describe the interplay between three sensory protein kinases in yeast: AMP-regulated kinase (AMPK, or SNF1 in yeast), PAS kinase 1 (Psk1 in yeast), and the target of rapamycin complex 1 (TORC1). This signaling cascade occurs through the SNF1-dependent phosphorylation and activation of Psk1, which phosphorylates and activates poly(A)- binding protein binding protein 1 (Pbp1), which then inhibits TORC1 through sequestration at stress granules. The SNF1-dependent phosphorylation of Psk1 appears to be direct, in that Snf1 is necessary and sufficient for Psk1 activation by alternate carbon sources, is required for altered Psk1 protein mobility, is able to phosphorylate Psk1 in vitro, and binds Psk1 via its substrate-targeting subunit Gal83. Evidence for the direct phosphorylation and activation of Pbp1 by Psk1 is also provided by in vitro and in vivo kinase assays, including the reduction of Pbp1 localization at distinct cytoplasmic foci and subsequent rescue of TORC1 inhibition in PAS kinase–deficient yeast. In support of this signaling cascade, Snf1-deficient cells display increased TORC1 activity, whereas cells containing hyperactive Snf1 display a PAS kinase–dependent decrease in TORC1 activity. This interplay between yeast SNF1, Psk1, and TORC1 allows for proper glucose allocation during nutrient depletion, reducing cell growth and proliferation when energy is low.**

Monitoring Editor
Daniel J. Lew
Duke University

Received: Jun 25, 2014
Revised: Oct 29, 2014
Accepted: Nov 16, 2014

INTRODUCTION

Nutrient-sensing kinases maintain metabolic homeostasis by allocating cellular resources in response to nutrient status. Their ability to control multiple central metabolic pathways has made them the target of many therapeutic approaches, including treatments for cancer and diabetes (Eglen and Reisine, 2011; Zhang and Daly, 2012; Fang *et al.*, 2013; Lal *et al.*, 2013; Rosilio *et al.*, 2014). This study focuses on the interplay between three evolutionarily conserved nutrient kinases—target of rapamycin complex 1 (TORC1), AMP-regulated kinase (AMPK, known as SNF1 in yeast), and PAS kinase (PASK, or Psk1 in yeast)—which all play critical roles in maintaining cellular homeostasis. TOR forms two distinct complexes in yeast and mammalian cells, TOR complex 1 (TORC1) and 2 (TORC2), and regulates cell growth and proliferation in response to a variety of signals, including nitrogen, amino acids, insulin, growth factors, and stress factors (due to the immense literature, only recent reviews are provided: Laplante and Sabatini, 2012; Porta *et al.*, 2014; Shimobayashi and Hall, 2014). AMPK/SNF1 regulates energy production and consumption pathways in response to the cellular AMP:ATP ratio. High AMP levels, which indicates low cellular energy, activate AMPK to stimulate energy production pathways and down-regulate energy consumption pathways (for recent reviews, see Ghillebert *et al.*, 2011; Broach, 2012; Hardie, 2013; Liu and Jiang, 2013; Burkewitz *et al.*, 2014; Rosilio *et al.*, 2014; Ye *et al.*, 2014). Mammalian PAS kinase is regulated by glucose levels and is essential for glucose homeostasis, specifically through the control of metabolic rate, insulin/glucagon secretion, and lipid/glycogen

This article was published online ahead of print in MBoC in Press (http://www.molbiolcell.org/cgi/doi/10.1091/mbc.E14-06-1088) on November 26, 2014.

Address correspondence to Julianne H. Grose (julianne_grose@byu.edu).

Abbreviations used: GFP, green fluorescent protein; Psk1, PAS kinase 1; Psk2, PAS kinase 2.

storage (da Silva Xavier *et al.*, 2004, 2011; Wilson *et al.*, 2005; An *et al.*, 2006; Hao *et al.*, 2007; Semplici *et al.*, 2011; Wu *et al.*, 2014). In yeast, there are two PAS kinase homologues, Psk1 and Psk2, which play a conserved role in the regulation of respiration and glycogen storage (Rutter *et al.*, 2002; Grose *et al.*, 2007, 2009; Smith and Rutter, 2007; DeMille *et al.*, 2014). These kinases coordinate cellular energy and nutrient availability with central metabolism, making cross-talk between these pathways essential for optimal cellular health.

The interplay between AMPK/SNF1 and TORC1 is documented in several studies. In mammals, activated AMPK inhibits TOR function through direct phosphorylation of the TORC1 subunit RAPTOR (Bolster *et al.*, 2002; Kimura *et al.*, 2003; Cheng *et al.*, 2004; Reiter *et al.*, 2005), as well as the phosphorylation and stabilization of tuberous sclerosis complex 2 (TSC2), a negative regulator of TORC1 (Inoki *et al.*, 2003a,b). This inhibition of TORC1 by AMPK appears to be conserved in yeast, in which glucose starvation has recently been shown to inhibit TORC1 in a SNF1-dependent manner (Hughes Hallett *et al.*, 2014).

There are also reported connections between PAS kinase, AMPK, and TORC1/2 in both mammalian and yeast cells. The TORC1 inhibitor TSC2 is activated by glycogen synthase kinase 3 (GSK3; Inoki *et al.*, 2003b, 2006), and GSK3 is in turn inhibited by PAS kinase–dependent phosphorylation (Semache *et al.*, 2013). These results suggest that PAS kinase may act as a progrowth signal in mammalian cells through the activation of TORC1. In support of this progrowth association, PAS kinase overexpression suppresses a temperature-sensitive mutation of TOR2 in yeast (*tor2ts*; Cardon *et al.*, 2012). In addition, PAS kinase was recently shown to be required for proper activation of AMPK and mTOR in the hypothalamus, where AMPK activation by nutrient depletion and TORC1 activation by refeeding are both blunted in PASK$^{-/-}$ mice (Hurtado-Carneiro *et al.*, 2013, 2014). The converse association is found in yeast, in which AMPK/SNF1 is required for the activation of PAS kinase by nonglucose carbon sources (Grose *et al.*, 2007). These studies solidify communication between AMPK, PAS kinase, and TORC1/2 and highlight the many overlapping complexities. Such overlap is expected to be extensive and complex, given the various mechanisms by which each kinase is activated and the importance of coordinating cellular energy and growth.

Here we provide molecular evidence for the Psk1-dependent interplay between AMPK/SNF1 and TORC1 in yeast. Both in vivo and in vitro assays support the direct phosphorylation and activation of Psk1 by Snf1. Once activated, Psk1 may phosphorylate poly(A)-binding protein binding protein 1 (Pab1 binding protein, or Pbp1), which is known to stimulate stress granule formation and inhibit TORC1 through sequestration (Takahara and Maeda, 2012). This phosphorylation is seen through direct in vitro phosphorylation assays, as well as in vivo phosphostate and phenotypic analysis. Finally, evidence is provided for the entire cascade, with SNF1 inhibiting TORC1 in a Psk1-dependent manner. Together these results support PAS kinase as a link between energy status and cell growth/proliferation, being activated by AMPK/SNF1 under nutrient/energy depletion and inhibiting cell growth/proliferation through the phosphorylation of Pbp1.

RESULTS

Evidence for in vivo phosphorylation and activation of Psk1 by SNF1

As mentioned, SNF1 is the master and commander of the fermentation/respiration switch in yeast and is required for the activation of Psk1 by nonglucose carbon sources (Grose *et al.*, 2007). We recently retrieved Snf1 and two of its subunits (Gal83 and Sip2) from a large-scale screen for Psk1 binding partners (DeMille *et al.*, 2014), suggesting that this activation is direct. To test for direct phosphorylation, in vivo Psk1 activity and phosphorylation state were monitored in response to SNF1 activation or depletion.

If this SNF1-dependent activation is due to direct phosphorylation rather than transcriptional regulation, the time required to activate Psk1 should be minimal. In support of direct in vivo phosphorylation, Psk1 was activated within 1 min of shifting cells from glucose to raffinose (Figure 1A), as determined by monitoring in vivo phosphorylation of the well-characterized substrate UDP-glucose pyrophosphorylase (Ugp1; Rutter *et al.*, 2002; Smith and Rutter, 2007; Grose *et al.*, 2009; Cardon *et al.*, 2012). To provide further in vivo evidence, Psk1 was purified from wild-type (WT), Snf1-deficient (*snf1*), and SNF1-hyperactive (*reg1*) yeast grown in galactose (to induce expression of Psk1 from the GAL1-10 promoter due to low endogenous levels), and analyzed by SDS–PAGE electrophoretic mobility shift assay (EMSA; Figure 1B). Reg1 is an inhibitor of SNF1 that promotes dephosphorylation by protein phosphatase 1 (Ludin *et al.*, 1998), making SNF1 constitutively active in Reg1-deficient yeast. An obvious mobility shift was observed between samples, indicating a SNF1-dependent protein modification. The shift is dramatic for such a large protein, suggesting a modification other than a single phosphorylation event. Mass spectrometry confirmed multisite phosphorylation. Samples from the WT, *reg1*, and *snf1* cells were submitted for mass spectrometry analysis and 17 phosphorylation sites were identified that appeared to be Snf1-dependent (S10, S101, S185, S202, S255, S307, T453, T496, T717, T919, S953, S992, S996, S1020, T1021, S1035, S1094). No other modifications were detected.

Evidence for direct phosphorylation and activation of Psk1 by Snf1

To determine whether the phosphorylation and activation of Psk1 is direct, we performed in vitro phosphorylation assays. Kinase-dead Psk1 (D1230A; DeMille *et al.*, 2014) was purified and subjected to in vitro kinase assays with purified Snf1. PAS kinase is known to autophosphorylate in vitro (Rutter *et al.*, 2001), making the kinase-dead mutant vital to ensure Snf1-dependent phosphorylation. Snf1-dependent Psk1 phosphorylation was seen in these in vitro assays (Figure 1C). These results confirm direct phosphorylation of Psk1 by Snf1.

PAS kinase contains a sensory N-terminal PAS domain and the C-terminal canonical serine/threonine kinase domain. In the model for PAS kinase regulation, the PAS domain binds and inhibits the kinase domain (Amezcua *et al.*, 2002). Phosphorylation of the PAS or kinase domain may disrupt such binding, activating the kinase. To determine domains necessary for Snf1-depedent phosphorylation, we used a truncated Psk1 bearing the kinase-only domain (ΔN931Psk1-KD [D1230A]; Figure 1C). Snf1 was able to phosphorylate even this kinase-only construct, suggesting that Snf1 phosphorylates Psk1 in the kinase domain. However, due to the large number of phosphorylation sites identified in the kinase domain (seven total), mapping the critical phosphorylation site(s) will require further study.

Evidence for an in vivo interaction between Psk1 and Snf1

As mentioned, Snf1 and two of its three β-subunits (Gal83 and Sip2) were retrieved as in vivo binding partners of Psk1 through copurification liquid chromatography–electrospray tandem mass spectrometry (LC–MS/MS) studies (DeMille *et al.*, 2014). An active SNF1 complex consists of three subunits: one of the three β-subunits (Gal83, Sip2, or Sip1), the Snf1 catalytic subunit, and the regulatory Snf4 subunit. Because copurification can retrieve large protein complexes, direct interaction between Psk1 and Snf1,

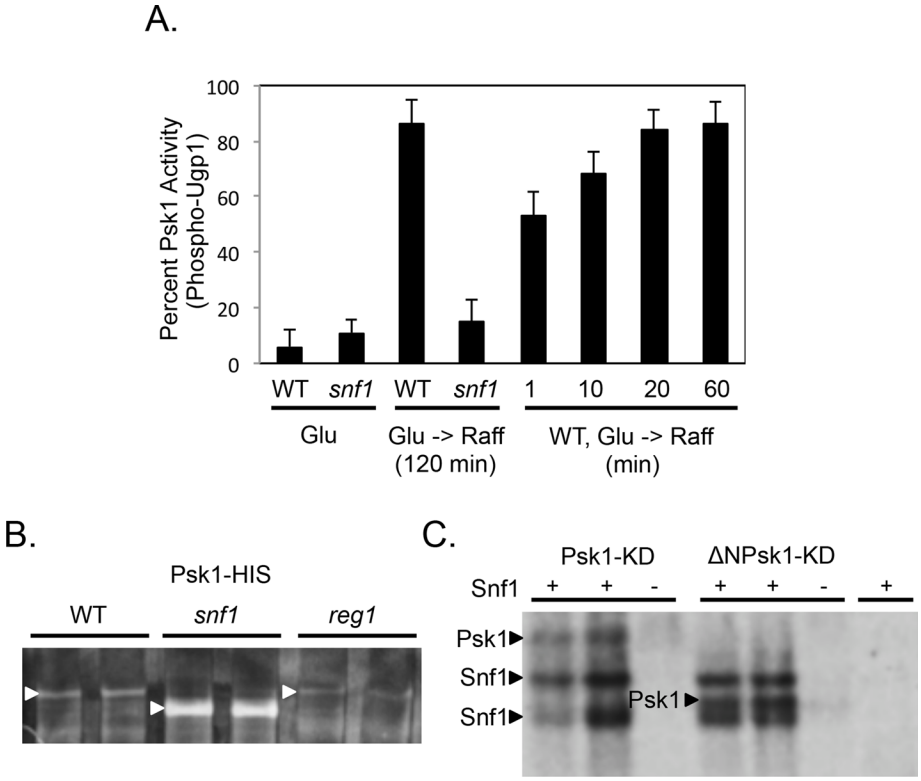

FIGURE 1: (A, B) In vivo and (C) in vitro evidence for Psk1 phosphorylation and activation by Snf1. (A) Psk1 is activated quickly by a nonfermenting carbon source in a Snf1-dependent manner. Yeast (*PSK1psk2*, JGY3) growing in YPAD (Glu) were transferred to a nonfermenting carbon source (YPA-raffinose, Raff) for the indicated time (minutes). Psk1 activity was measured by assessing Ugp1 phosphorylation in crude yeast extracts by a monoQ fractionation as previously described (Smith and Rutter, 2007). (B) Psk1 protein displays a gel shift when purified from cells expressing Snf1. HIS-HA epitope-tagged Psk1 was purified from WT, Snf1-deficient (*snf1*), and SNF1-hyperactive (*reg1*) cells grown in galactose, analyzed by 8% SDS–PAGE, and visualized by silver stain. (C) Snf1 directly phosphorylates Psk1 in vitro. Full-length (Psk1-KD [D1230A]) and truncated (ΔN931Psk1-KD [D1230A]) kinase-dead Psk1 were incubated with Snf1 and ^{32}P-ATP. Autoradiograms of SDS–PAGE gels are shown, and Snf1-dependent incorporation of ^{32}P-ATP is seen in both Psk1 constructs. Kinase-dead Psk1 was used to prevent autophosphorylation. Coomassie blue–stained gels are not shown due to low protein expression, making it difficult to visualize by staining, but all proteins are the expected size.

Gal83, or Sip2 was examined via the yeast two-hybrid (Y2H) system. All three proteins were cloned into both the Y2H prey and bait plasmids (James *et al.*, 1996) and tested for interaction using a Psk1 bait or prey plasmid, respectively (Figure 2A). The Y2HGold strain was used, which harbors four different reporters (ADE2, HIS3, AUR1-C, MEL1) under three different Gal4-responsive promoters (Clontech), and transformed yeast were spotted onto selective media for protein–protein interactions, as well as for plasmid maintenance (media lacking histidine and adenine, as well as tryptophan and leucine, respectively). Note that all constructs were tested with their corresponding empty vector control and were negative. A direct interaction was detected between Psk1 and Gal83 but not Sip2 or Snf1. These results are not surprising, given that the Gal83 and Sip2 β-subunits of Snf1 are each responsible for binding a subset of its targets (Vincent and Carlson, 1999; Schmidt and McCartney, 2000). Whereas a strong interaction was seen between Psk1 and Gal83 when Gal83 was used as the bait, no interaction was observed when Gal83 was used as the prey, suggesting a nonfunctional construct. The Psk1/Gal83 interaction was also strong when using either full-length Psk1 or a truncation removing the PAS domain (ΔN692Psk1). This interaction supports the in vitro phosphorylation of the kinase-only Psk1 construct observed in Figure 1C.

Previous Y2H interactions of Psk1 with its substrates were detected using the ΔN692Psk1 but not the full-length Psk1 construct (DeMille *et al.*, 2014). The Psk1/Gal83 interaction is different, in that both full-length and truncated Psk1 bound Gal83. This finding lends additional support for Psk1 being a substrate of SNF1 rather than an upstream kinase.

The Gal83 protein was then truncated to determine the regions required for interaction with Psk1 (Figure 2, B and C). Gal83 has three main regions: an N-terminal region containing a glycogen-binding domain (amino acids [aa] 1–141), which has been shown to mediate the interaction between Snf1 and Reg1 (Momcilovic *et al.*, 2008); a "Snf1-binding domain" (aa 141–343); and a C-terminal "Snf4-interacting domain" (aa 343–417; Jiang and Carlson, 1997). The Gal83 Snf1-binding domain was clearly necessary for the Gal83 Psk1 interaction (Figure 2C). This direct in vivo interaction, combined with the foregoing in vivo and in vitro phosphorylation and activation assays, affords strong evidence for the direct phosphorylation and activation of Psk1 by Snf1.

Evidence for direct phosphorylation of Pbp1 by Psk1

In addition to Snf1 and its subunits, Pbp1 was recently identified as a Psk1 binding partner (DeMille *et al.*, 2014). Although Pbp1 was retrieved from both yeast two-hybrid and copurification screens, we did not observe phosphorylation of full-length Pbp1 when purified from bacteria (DeMille *et al.*, 2014) or yeast (unpublished data). However, the Y2H retrieved two truncations of Pbp1 (ΔN196Pbp1 and ΔN355Pbp1), and when a further truncated (ΔN419Pbp1) Pbp1 was used in the in vitro kinase assays, a strong phosphorylation was observed (Figure 3A). The ability of Psk1 to phosphorylate the truncated but not full-length Pbp1 suggests that Pbp1 may adopt different conformations regulated by its N-terminal end.

Pbp1 contains three regions: the Sm domain, the LSmAD domain, and the self-interaction region (Figure 3B). The Sm (Sm-ATX or LSm) domain is required for interaction with other proteins, namely Lsm12, Pbp4, and Rpl12a. The LSmAD domain is usually associated with Sm domains and enhances protein binding, and the self-interaction region is required for binding Pab1 and itself (Mangus *et al.*, 2004; Kimura *et al.*, 2013). To map the Pbp1 regions necessary for Psk1 interaction, we tested several Pbp1 truncations via the Y2H assay (Figures 3, B and C; note that all constructs were tested with their corresponding empty vector control and were negative). The results mirrored the in vitro kinase assays, in that Psk1 was not able to bind the full-length Pbp1 protein but bound truncated constructs in which the N-terminal 196 amino acids were removed. Larger N-terminal truncations were made to further characterize the minimal region necessary for interaction.

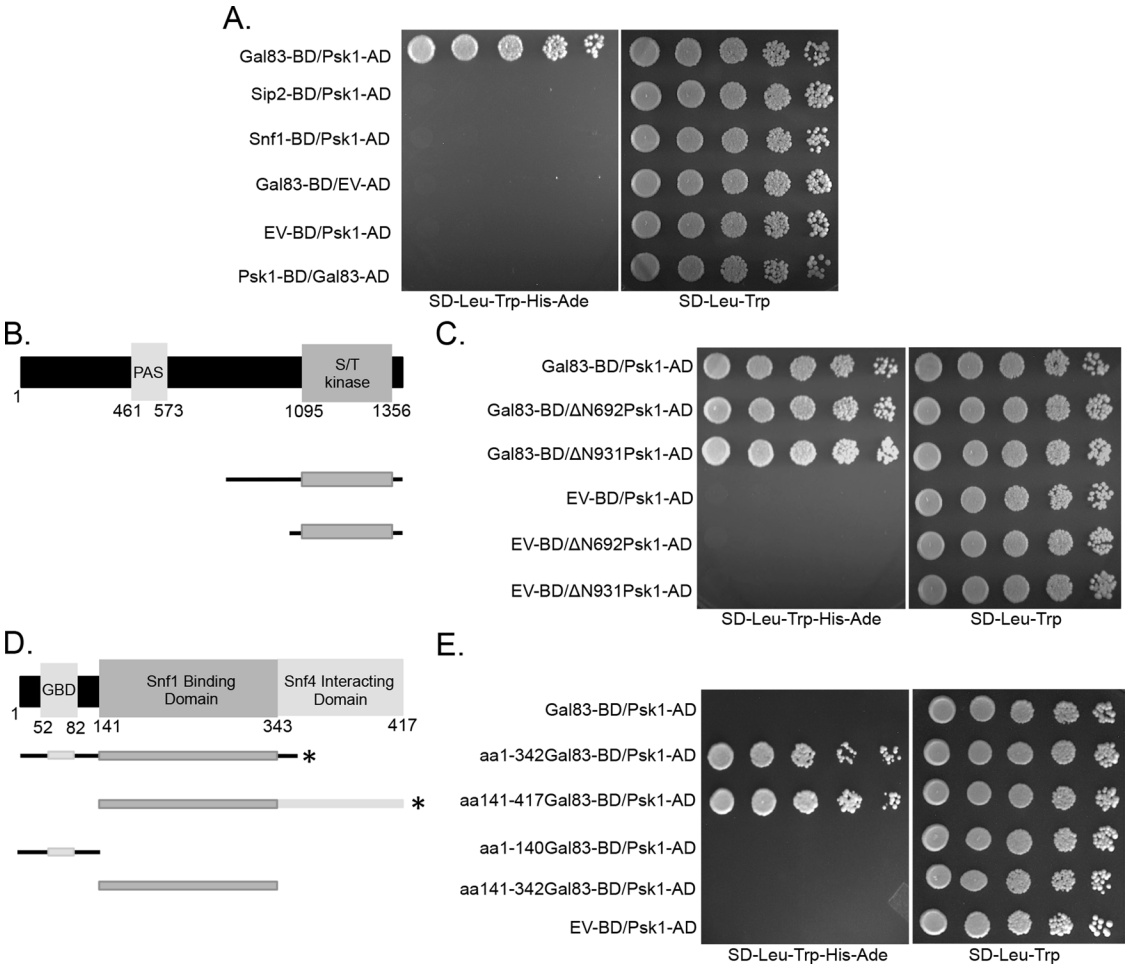

FIGURE 2: Yeast two-hybrid assays reveal an interaction between the Gal83 Snf1-binding domain and the Psk1 kinase domain. (A) The SNF1 complex subunit Gal83, but not Sip2 or Snf1, interacts with full-length Psk1. Y2HGold cells (Clontech) containing the Gal83 (pJG1236 or pJG1237), Sip2 (pJG1238 or pJG1239), and Snf1 (pJG1240 or pJG1241) bait (BD) and prey (AD) plasmids, respectively, were cotransformed with bait and prey plasmids harboring full-length Psk1 (pJG441 or pJG442) or empty vector (pJG424 or pJG421). Only representative interactions are shown (all other combinations of bait and prey were negative). (B) Psk1 truncations used to screen for interactions with Gal83 are diagrammed. (C) Gal83 interacts with truncated versions of Psk1 that harbor the kinase domain. Y2HGold cells were cotransformed with bait plasmids harboring either Gal83 (pJG1236) or the empty vector (pJG424), and prey plasmids harboring truncations of Psk1 (ΔN692Psk1 [pJG709] or ΔN931Psk1 [pJG1276]). (D) The Snf1-binding domain is necessary for interaction with Psk1. Truncations used to screen for the Gal83 domains necessary for Psk1 binding are diagrammed. Constructs are marked with an asterisk if any binding to Psk1 was detected in the Y2H assays shown in E. (E) Y2HGold cells containing the Psk1 prey plasmid (pJG442) were cotransformed with bait plasmids harboring full-length Gal83 (pJG1236), truncated Gal83 (aa 1–342 [pJG1258], 141–417 [pJG1260], 1–140 [pJG1262], 141–342 [pJG1264]), or empty vector (pJG424). Overnight samples were grown in SD-Leu-Trp for plasmid maintenance, diluted fivefold serially, and plated on Y2H selective medium (SD-Leu-Trp-His-Ade), as well as on a control plate (SD-Leu-Trp). Plates were incubated at 30°C for 3–4 d.

Removal of the N-terminal 419 amino acids still allowed for a Psk1 interaction, whereas removal of the N-terminal 469 amino acids did not. Further attempts to narrow in on the essential interaction region of Pbp1 by creating C-terminal truncations in the self-interaction domain (removing aa 420-722, 566–722, 581–722, or 661–722) did not result in constructs that interact, even when the N-terminus was also removed. Thus the Pbp1 self-interaction region (aa 420–722) is necessary for in vivo association with Psk1, whereas the N-terminal Sm region (aa 1–197) of Pbp1 appears to inhibit interaction. Because this C-terminal region is involved in enhancing protein binding (Mangus *et al.*, 2004; Kimura *et al.*, 2013), the phosphorylation of Pbp1 by Psk1 may either enhance or inhibit its activity.

Evidence for in vivo phosphorylation and activation of Pbp1 by Psk1

The combined evidence of in vivo protein–protein interaction with in vitro kinase assays makes Pbp1 a high-confidence cellular Psk1 substrate. To determine whether Pbp1 is phosphorylated by Psk1 in vivo, we monitored the Psk1-dependent phosphorylation of Pbp1 through nonspecific PhosphoThreonine (Cell Signaling Technology) or PhosphoSerine (Q5; Qiagen) antibodies (Figure 4A). HIS-HA epitope-tagged Pbp1 was purified from yeast grown on galactose, and a Western blot revealed Psk1-dependent phosphorylation of at least one threonine residue, whereas phosphoserine presence was independent of Psk1. Phosphorylation state was assessed in cells deficient in both Psk1 and Psk2 *(PSK1PSK2* deficient) as compared with

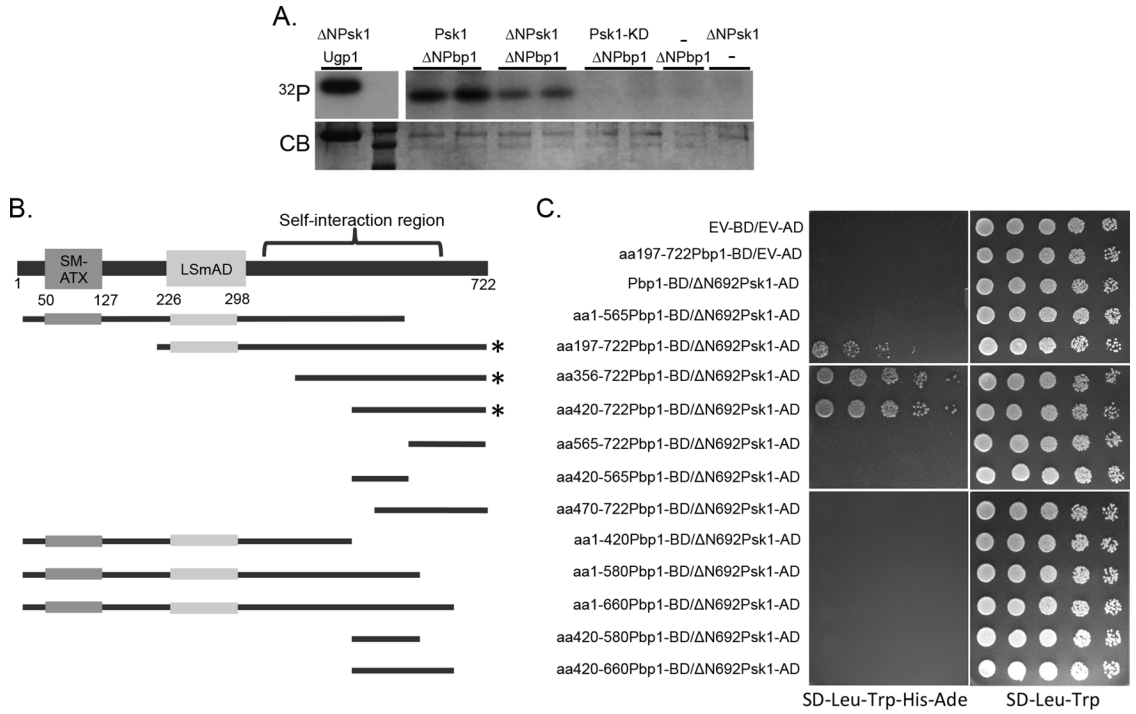

FIGURE 3: Evidence for direct phosphorylation of Pbp1 by Psk1. (A) Truncated Pbp1 (ΔN419Pbp1, aa 420–722, pJG1250) was shown to be phosphorylated in vitro when incubated in the presence of either full-length (pJG1181) or truncated (ΔN931Psk1, pJG1216) Psk1 but not with the kinase-dead mutant (Psk1-KD, pJG1215). In vitro kinase assays using purified Pbp1 protein incubated with radiolabeled ATP (^{32}P) in the presence or absence of purified Psk1. Reactions were visualized on 15% SDS–PAGE gels, stained with Coomassie brilliant blue (CB; bottom), and exposed on x-ray film (^{32}P; top). Ugp1 (a positive control) and Pbp1 were run on the same gel, but the film was developed differently due to varying signal strength. (B) A diagram of the Pbp1 protein, including the conserved domains. The C-terminal portion of the protein is known as the self-interaction region. The Pbp1 truncations tested in the yeast two-hybrid are diagrammed, and those that interacted with Psk1 are marked with an asterisk. (C) Mapping the Psk1-binding region of Pbp1 reveals an inhibitory N-terminus and a required C-terminal region between aa 420 and 722. The Y2H prey vector containing full-length Pbp1 (pJG1008), Pbp1 truncations (aa 1–565 Pbp1 [pJG1168], 197–722 Pbp1 [pJG1002], 356–722 Pbp1 [pJG1001], 420–722 Pbp1 [pJG1003], 565–722 Pbp1 [pJG1004], 420–565 Pbp1 [pJG1169], 470–722 Pbp1 [pJG1195], 1–420 Pbp1 [pJG1196], 1–580 Pbp1 [pJG1197], 1–660 Pbp1 [pJG1198], 420–580 Pbp1 [pJG1230], and 420–660 Pbp1 [pJG1231]) or empty vector (EV, pJG423) were expressed in yeast (JGY1031) along with the empty vector (EV, pJG425) or ΔN692Psk1 (pJG598) bait plasmid. Overnight samples were grown in SD-Leu-Trp for plasmid maintenance, diluted fivefold serially, and plated on Y2H selective medium (SD-Leu-Trp-His-Ade), as well as on a control plate (SD-Leu-Trp). Plates were grown at 30°C for 2–5 d.

WT because both Psk1 and Psk2 phosphorylate the well-characterized PAS kinase substrate Ugp1. Psk2 is unlikely to phosphorylate Pbp1 in this study, however, because Psk2 is not expressed on carbon sources other than glucose, and is thus not activated by Snf1 (Grose *et al.*, 2007). Therefore phosphorylation of Pbp1 grown in galactose is attributed to Psk1 activity.

To determine the effects of this phosphorylation on Pbp1 function, Pbp1-dependent caffeine sensitivity was assessed in WT and *PSK1PSK2*-deficient yeast. Pbp1 has been shown to inhibit TORC1 through its sequestration to stress granules (Takahara and Maeda, 2012), suggesting a role for PAS kinase in TORC1 regulation. This sequestration and inactivation of TORC1 produces a caffeine sensitive phenotype. *PSK1PSK2* deficiency alleviates the caffeine sensitivity of cells overexpressing *PBP1*, consistent with Psk1-dependent activation of Pbp1 (Figure 4B). Combined these results suggest that Psk1 phosphorylates Pbp1 at a threonine residue, which activates Pbp1, inducing stress granule formation and subsequent TORC1 sequestration.

Psk1 increases Pbp1 localization at cytoplasmic foci

The Pbp1-dependent localization of TORC1 to stress granules was previously shown by Takahara and Maeda (2012). To determine whether Psk1 also localizes to the same distinct cytoplasmic foci as Pbp1, red fluorescent protein (RFP)–tagged Psk1 was transformed into yeast containing Pbp1–green fluorescent protein (GFP). Cytoplasmic foci were induced by glucose deprivation, a condition known to induce both P-body and stress granule formation. Psk1 colocalized to distinct cytoplasmic foci with Pbp1 in ~74% of cells in which Pbp1-GFP foci were visible (Figure 4C).

The effect of PAS kinase on Pbp1 localization to distinct foci was then assessed. Pbp1-GFP foci were significantly reduced in the *psk1psk2* yeast when compared with WT (Figure 4D), suggesting that PAS kinase activates Pbp1 by increasing localization to stress granules or P-bodies.

Snf1 inhibits TORC1 phosphorylation of Sch9

We provided evidence for the Snf1-dependent phosphorylation and activation of Psk1, which then leads to the phosphorylation and activation of Pbp1, inhibiting TORC1. To further support this model, we monitored TORC1 activity in response to both Snf1 and PAS kinase. TORC1 activity was assessed through the in vivo phosphostate of the S6 kinase, Sch9, commonly used as a readout of TORC1 activity (Kingsbury *et al.*, 2014; Urban *et al.*, 2007). Sch9 is phosphorylated

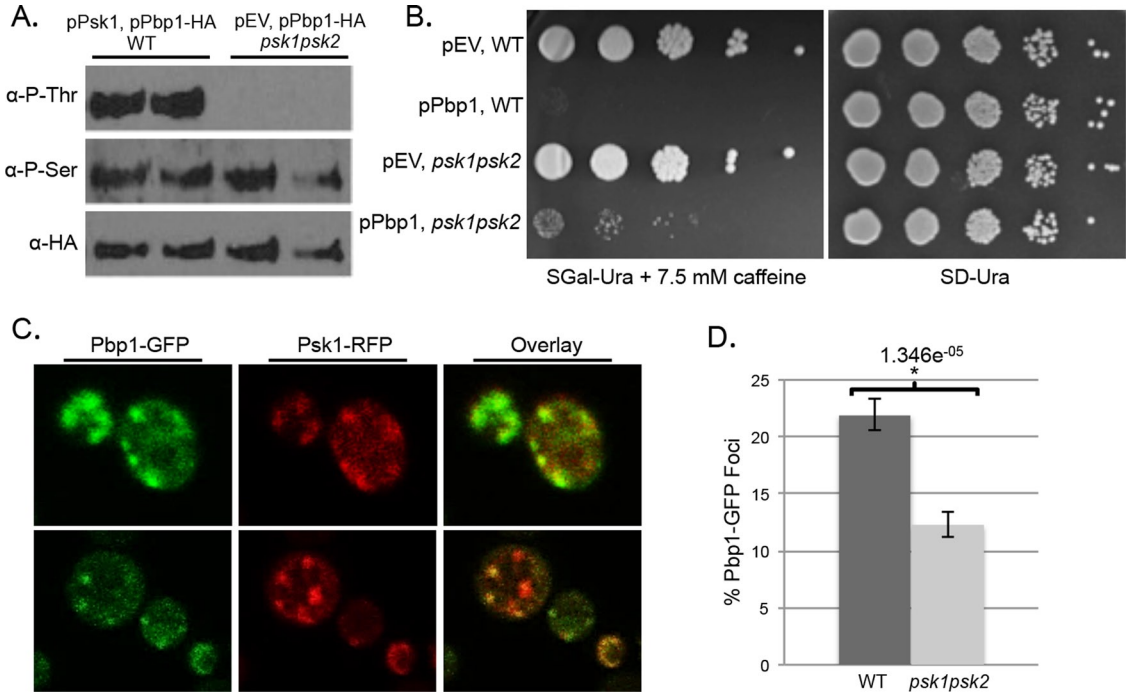

FIGURE 4: In vivo evidence for the activation of Pbp1 by Psk1. (A) Monitoring the in vivo phosphorylation state of Pbp1 reveals Psk1-dependent threonine phosphorylation. Purified HIS-HA epitope-tagged Pbp1 protein from WT cells (JGY1) overexpressing full-length Psk1 (pJG9) was compared with purified Pbp1 from *PSK1PSK2*-deficient cells (*psk1psk2,* JGY4) using anti-PhosphoThreonine (Cell Signaling Technology) and anti-PhosphoSerine antibodies (Q5; Qiagen). Anti-HA antibody (Roche) was used as a control for total Pbp1 protein. (B) *PSK1PSK2* deficiency ameliorates caffeine toxicity due to Pbp1 overexpression. Wild-type (JGY299) or *psk1psk2* yeast (JGY1161) was transformed with an empty vector (EV, pJG859) or a plasmid overexpressing Pbp1 (pJG925), grown in SD-Ura, serially diluted 1:10, and spotted on SGal-Ura + 7.5 mM caffeine plates, as well as on a control SD-Ura plate. Plates were incubated at 30°C for 7–10 d until colonies were apparent. (C) Colocalization of Psk1 and Pbp1 to stress granules. Pbp1-GFP fusion yeast (Invitrogen) was transformed with Psk1-RFP (pJG1119), grown under glucose deprivation (SC medium lacking a carbon source), and imaged using an Olympus Fluoview confocal microscope. (D) Pbp1-GFP foci decrease significantly in *psk1psk2* (JGY1160) yeast compared with WT (JGY1144). For percentage of Pbp1-GFP foci, 1199 cells for WT and 782 for *psk1psk2* were counted. SEM was used for error bars, and Student's *t* test was used in statistical significance calculations.

on glucose, and Snf1 is necessary and sufficient for its dephosphorylation, as shown through the increased phosphorylation seen in the Snf1-deficient strain (*snf1*) and the dramatic decrease seen in the hyperactive Snf1 strain (*reg1*; Figure 5). In addition, PAS kinase was shown to be essential for this apparent inhibition of TORC1, as seen by dramatic increase in phosphorylation in *reg1* or *reg1snf1* yeast that are also Psk1Psk2 deficient.

DISCUSSION

The nutrient-sensing protein kinases TOR (which forms the TORC1 and TORC2 complexes) and AMPK/SNF1 are essential regulators of growth/proliferation and cellular energy, respectively. Several studies have shown the interplay between these kinases, including the direct phosphorylation and inhibition of mammalian TORC1 by AMPK (Bolster *et al.*, 2002; Kimura *et al.*, 2003; Cheng *et al.*, 2004; Reiter *et al.*, 2005). This study provides evidence for PAS kinase as a mediator in the inhibition of TORC1 by Snf1 in yeast (Figure 6).

In yeast, Psk1 is activated in a SNF1-dependent manner in response to energy/nutrient deprivation (Grose *et al.*, 2007). This study expands these findings by providing in vivo and in vitro evidence for the direct phosphorylation and subsequent activation of Psk1 by Snf1 (Figure 1). Phosphorylation may activate PAS kinase by interfering with inhibitory binding of the PAS domain. Once activated, Psk1 phosphorylates Pbp1 (Figures 3 and 4), which sequesters TORC1 to stress granules, inhibiting cell growth (Takahara and Maeda, 2012). Caffeine sensitivity is associated with inhibition of TORC1, and Psk1Psk2 deficiency can rescue the caffeine sensitivity of cells overexpressing Pbp1 (Figure 4B), suggesting that phosphorylation of Pbp1 by Psk1 is activating. In support of this finding, Psk1Psk2 deficiency reduces the amount of Pbp1 localized to distinct cytoplasmic foci (Figure 4D).

This model for the PAS kinase–dependent interplay between SNF1 and TORC1 was further supported by monitoring the in vivo phosphorylation state of Sch9, a TORC1 substrate. Sch9 was fully phosphorylated in WT yeast grown on glucose. This phosphorylation was increased in *snf1* yeast and inhibited in *reg1* yeast, in which Snf1 is constitutively active (Figure 5). In addition, PAS kinase was necessary for this inhibition. During the revision of the manuscript, an article was published validating the Snf1-dependent inhibition of TORC1 signaling on alternate carbon sources (Hughes Hallett *et al.*, 2014). Our results describe the molecular pathways underlying this observation.

The present article describes the second recent connection between yeast PAS kinase and TOR. In yeast, two TOR paralogues exist, Tor1 (which is a subunit of TORC1) and Tor2 (which can function in both TORC1 and TORC2 complexes). TORC1 primarily controls growth in response to nutrients through the regulation of transcription, translation, ribosome biogenesis, nutrient transport, and autophagy; TORC2 controls cell cycle–dependent polarization of the actin cytoskeleton (for a review, see Loewith and Hall, 2011).

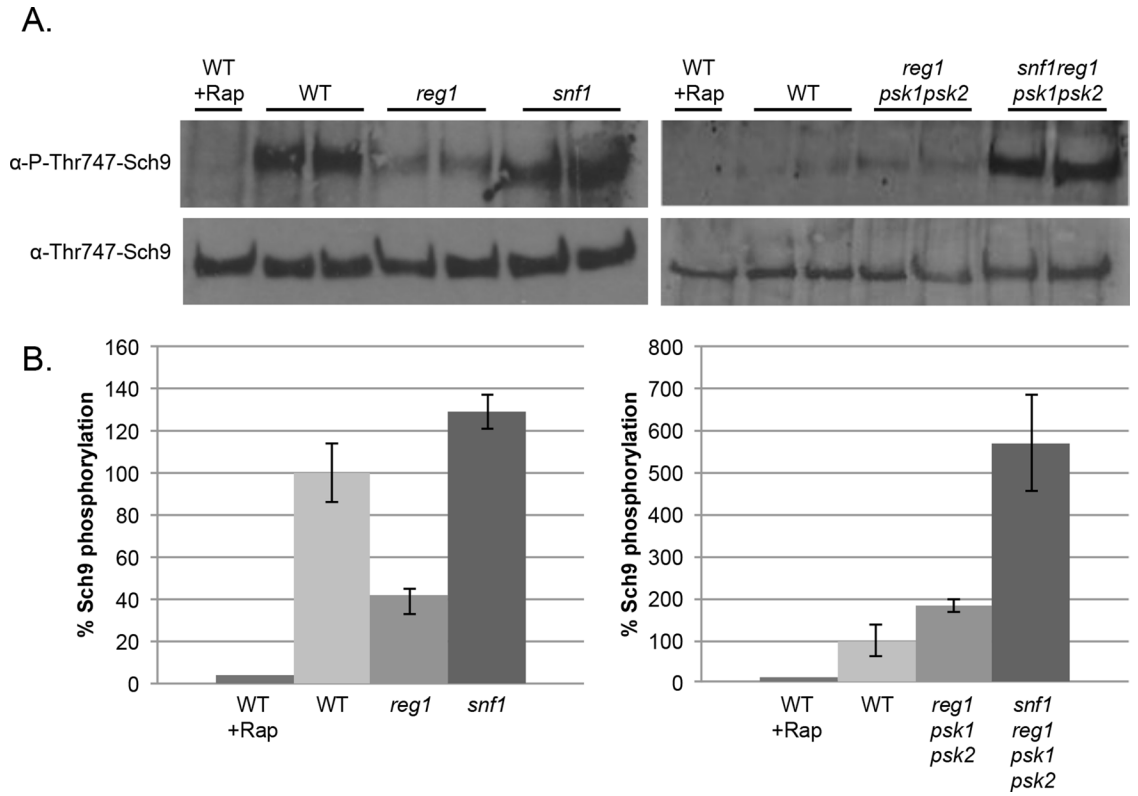

FIGURE 5: SNF1 inhibits TORC1 phosphorylation of Sch9 through PAS kinase. (A) Western blots of phospho-Sch9 and total Sch9. (B) Quantification of band intensities in A. A plasmid expressing Sch9 under the yeast ADH promoter was transformed into yeast (WT [JGY1], *reg1* [JGY95], *snf1* [JGY91], *reg1psk1psk2* [JGY283], *reg1snf1psk1psk2* [JGY280]). Yeast were grown in YPAD until OD_{600} ~1.0. Preparation of Sch9 protein extract was performed as described by Miller-Fleming *et al.* (2014). Samples were normalized and loaded on 8% SDS–PAGE, transferred to nitrocellulose membrane, and incubated overnight with anti–phospho-Thr737-Sch9 and anti–Thr737-Sch9 antibodies (Kingsbury *et al.*, 2014). Intensity signals were quantified using ImageJ. Phosphorylation was determined in duplicate. Error bars represent SEM.

Overexpression of yeast *PSK1 or PSK2* suppresses a *tor2ts* mutation (Cardon *et al.*, 2012; Cardon and Rutter, 2012), suggesting rescue of the TORC2 complex, since TORC1 is still functional in this background. In contrast, Psk1 appears to be a negative regulator of TORC1 activity (Figures 4 and 5). These findings are consistent with the cellular selection for two differentially controlled TOR complexes that regulate separate pathways involved in cell growth and proliferation.

In a cell's adaptation to its environment, there cannot simply be one "progrowth" pathway, but instead alternate pathways, such as those allowing for growth with or without division. Not only are there separate TOR complexes, but these complexes regulate different pathways in response to different stimuli. This complexity is necessary due to the multiple metabolic inputs and outputs the cell must sense (e.g., energy, amino acids, nitrogen, carbon source, etc.). It remains to be determined whether PAS kinase inhibits only the phosphorylation of Sch9, a progrowth kinase stimulating many pathways including protein synthesis, or whether other TORC1 pathways are also affected. The PAS kinase–dependent interplay between SNF1 and TORC1 would allow for an additional regulatory input, rather than just direct SNF1-dependent phosphorylation of TORC1.

The complexity of these pathways is further demonstrated by comparing different cell types. Although the direct inhibition of TORC1 by AMPK reported in mammalian cells (Bolster *et al.*, 2002; Kimura *et al.*, 2003; Cheng *et al.*, 2004; Reiter *et al.*, 2005) is consistent with the overall pathway mediated by PAS kinase described here, PAS kinase is predicted to activate TORC1 in mammalian cells through the inhibition of GSK3 (Inoki *et al.*, 2003b, 2006; Semache *et al.*, 2013). This alternate role for PAS kinase may be due to the differential metabolic responses of different cell types. For example, yeast ferment when glucose is high and respire on poor carbon sources, whereas mammalian cells activate respiration in response to nutrient-rich conditions (high glucose). These differences are reflected in AMPK/SNF1 activity, which is stimulated by alternate carbon sources in yeast and high glucose in mammalian cells (Ghillebert *et al.*, 2011; Broach, 2012; Hardie, 2013; Liu and Jiang, 2013; Burkewitz *et al.*, 2014; Ye *et al.*, 2014). Whether PAS kinase also mediates inhibition of TORC1 through the mammalian Pbp1 homologue, ataxin-2, remains to be seen.

These findings may provide valuable insight into the function of PAS kinase in mammalian cells, in that all of the proteins in this pathway have conserved homologues. The human homologue of Pbp1, ataxin-2, is associated with neurodegenerative disease. This study provides both in vitro and in vivo evidence for the direct, Psk1-dependent phosphorylation of Pbp1 and the inhibition of phosphorylation by the Pbp1 N-terminal domain (Figure 3). This N-terminal truncation may trap Pbp1 into a conformation that is naturally obtained under certain in vivo conditions because WT Pbp1 copurifies with Psk1 (DeMille *et al.*, 2014) and is phosphorylated in a Psk1-dependent manner within cells (Figure 4A). The N-terminus of Pbp1, which inhibits Psk1-dependent phosphorylation, also harbors the ataxin-2 domain, a conserved domain required for localization to

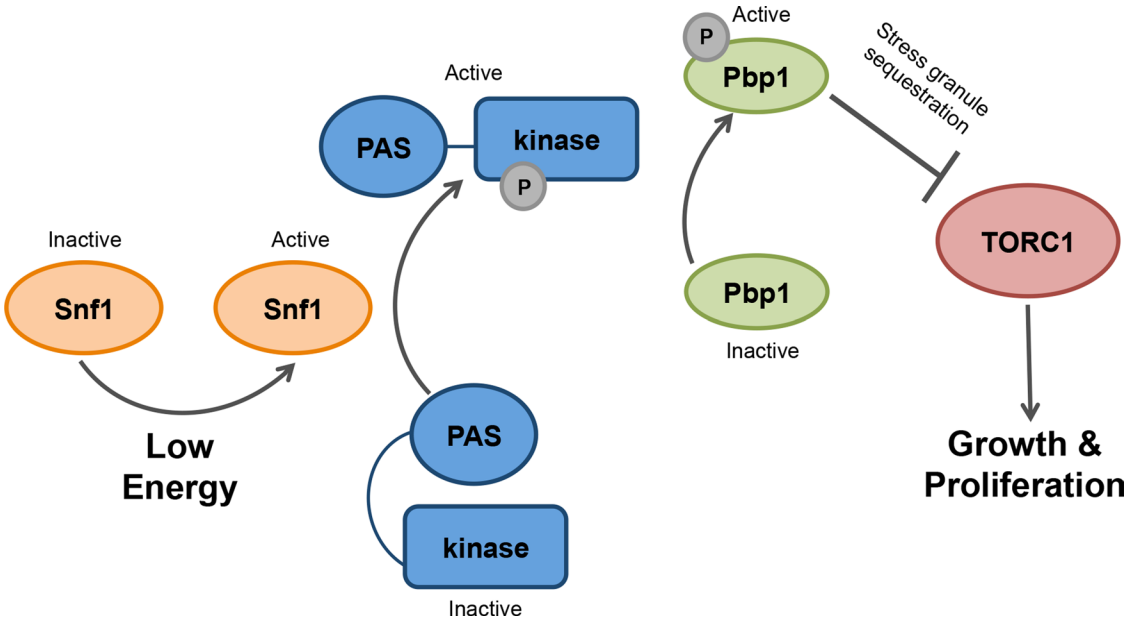

FIGURE 6: A model for the cross-talk between the nutrient-sensing kinases SNF1, TORC1, and Psk1 proposed in this study. SNF1 becomes activated when cellular energy levels are low (such as in conditions of glucose deprivation) and phosphorylates PAS kinase (Psk1). This phosphorylation leads to a disruption of the inhibitory binding of the PAS domain, leading to activation of the kinase. Once active, Psk1 phosphorylates Pbp1, which inhibits TORC1 by sequestering it to stress granules. The inhibition of TORC1 inactivates the S6 kinase, Sch9, and possibly other pathways that control cellular growth and proliferation.

P-bodies and stress granules and for promoting their formation (Mangus *et al.*, 1998; Nonhoff *et al.*, 2007; Swisher and Parker, 2010; Kaehler *et al.*, 2012). The conservation of this N-terminal domain suggests that this regulatory role may also be conserved. Because mutations in ataxin-2 are associated with cerebral ataxia (SCA2), amyotrophic lateral sclerosis (ALS), and parkinsonism (for recent reviews, see Magana *et al.*, 2013; Borza, 2014), understanding the regulation of this protein may provide key therapeutic targets for disease treatment.

The cross-talk between AMPK/SNF1, PAS kinase, and TOR seems vital for appropriate metabolic regulation, linking energy production to growth in response to a wide variation in available nutrients. These pathways are central to understanding a cell's basic metabolism. In addition, both AMPK and TOR are key therapeutic targets for the treatment of a variety of diseases, including obesity, diabetes, and cancer (for recent reviews, see Khan *et al.*, 2013; Quinn *et al.*, 2013). As a nonessential protein, PAS kinase may prove to be a safer target for therapeutic treatment of metabolic disease.

MATERIALS AND METHODS

Growth assays

Lists of strains, plasmids, and primers used in this study are provided in Table 1. For plasmid construction, standard PCR-based cloning methods were used. All restriction enzymes were purchased from New England BioLabs (Ipswich, MA). Yeast two-hybrid bait and prey plasmids were made by PCR amplification and subsequent cloning into the *Eco*RI/*Sal*I sites of pJG424 (pJG1236 [JG3199/3200], pJG1238 [JG3245/3246], pJG1240 [JG3274/3275], pJG1258 [JG3199/3532], pJG1260 [JG3531/3200], pJG1262 [JG3199/3530], pJG1264 [JG3531/3532]) or the *Eco*RI/*Sal*I sites of pJG421 (pJG1003 [JG3136/3138], pJG1004 [JG3137/3138], pJG1008 [JG2916/2917], pJG1168 [JG2917/3418], pJG1169 [JG3419/3418], pJG1195 [JG3460/3138], pJG1196 [JG2917/3461], pJG1197 [JG2917/3462], pJG1198 [JG2917/3463], pJG1230 [JG3136/3462], pJG1231 [JG3136/3463], pJG1237 [JG3199/3200], pJG1239 [JG3245/3246], pJG1241 [JG3274/3275], pJG1259 [JG3199/3532], pJG1261 [JG3531/3200], pJG1262 [3530/3199], pJG1263 [JG3199/3530], pJG1265 [JG3531/3532], pJG1276 [2454/2458]). Two constructs were retrieved from an earlier Y2H screen and were not made by PCR (pJG1001 and pJG1002; DeMille *et al.*, 2014). Yeast two-hybrid Gold cells (Clontech, Mountain View, CA) were used to transform in bait and prey plasmids for interaction studies.

For yeast-two hybrid spot dilutions, overnight samples were grown in selective SD-Leu-Trp media, serially diluted 1:5 in water and spotted to SD-Leu-Trp-His-Ade or SD-Leu-Trp plates as a control, and incubated at 30°C for 2–5 d until colonies were apparent. For caffeine sensitivity assays, spot dilutions were performed by growing overnight samples in SD-Ura media, diluting saturated overnights 1:10 in water, and spotting on SGal-Ura media with 7.5 mM caffeine or SD-Ura as a control. Plates were incubated at 30°C for 7–10 d.

Histidine- and Myc-tagged protein purification

Yeast harboring plasmids for histidine (HIS)- or Myc-tagged protein expression were grown in SD-Ura media overnight, diluted 1:100-fold into 100 or 500 ml of SD-Ura, and grown for 10–12 h, pelleted, and resuspended in SGal-Ura for 36 h to induce expression under the GAL1-10 promoter. Yeast were pelleted and resuspended in lysis buffer for HIS purification (50 mM 4-(2-hydroxyethyl)piperazine-1-ethanesulfonic acid [HEPES], 300 mM NaCl, 20 mM imidazole, 10 mM KCl, 1 mM β-mercaptoethanol, and 1:300 mammalian protease inhibitor cocktail [Sigma-Aldrich, St. Louis, MO] or cOmplete Protease Inhibitor Cocktail Tablet [Roche], pH 7.8, with phosphatase inhibitors, 50 mM NaF, and glycerophosphate when necessary) or for Myc purification (20 mM HEPES, 10 mM KCl, 1 mM EDTA, 1 mM ethylene glycol tetraacetic acid [EGTA], 50 mM NaCl, 10% glycerol,

Strain	Background	Genotype	Abbreviation	a/α	Reference or source
JGY1	W303	*ade2-1 can1-100 his3-11,15 leu2-3112 trp1-1 ura3-1*	WT	a	David Stillman (University of Utah, Salt Lake City, UT)
JGY3	W303	*psk2*::kan-MX4 *ade2-1 can1-100 his3-11,15 leu2-3112 trp1-1 ura3-1*	*PSK1psk2*	a	Grose *et al.* (2007)
JGY4	W303	*psk1*::*his3 psk2*::kan-MX4 *ade2-1 can1-100 his3-11,15 leu2-3112 trp1-1 ura3-1*	*psk1psk2*	a	Grose *et al.* (2007)
JGY91	W303	*snf1*::hphMX4 *ade2-1 can1-100 his3-11,15 leu2-3112 trp1-1 ura3-1*	*snf1*	a	Grose *et al.* (2007)
JGY95	W303	*reg1*::hphMX4 *ade2-1 can1-100 his3-11,15 leu2-3112 trp1-1 ura3-1*	*reg1*	a	Grose *et al.* (2007)
JGY299	S288C	*PSK2*-TAPtag::kanMX *ura3-0 trp1-0 SUC2 mal mel gal2 CUP1 flo1 flo8-1*	WT	α	Jared Rutter (University of Utah, Salt Lake City, UT)
JGY280	W303	*psk1*::*HIS3 psk2*::*kanMX4 reg1*::*hphMX4 snf1*::*URA3 ade2-1 can1-100 his3-11,15 leu2-3112 trp1-1 ura3-1*	*snf1reg1 psk1psk2*	a	Jared Rutter
JGY283	W303	*psk1*::*HIS3 psk2*::*kanMX4 reg1*::*hphMX4 ade2-1 can1-100 his3-11,15 leu2-3112 trp1-1 ura3-1*	*reg1psk1p-sk2*	a	Jared Rutter
Y2H Gold (JGY1031)		*LYS2*::*GAL1*UAS-*GAL1*TATA-His3, *GAL2*UAS-Gal2TATA-Ade2 *URA3*::*MEL1*UAS-*MEL1*TATA, *AUR1-CMEL1*, *ura3-52 his3-200 ade2-101 trp1-901 leu2-3, 112 gal4del gal80del met-*	Y2H Gold	a	Clontech
JGY1144	BY4741	Chromosomally-tagged Pbp1-GFP::*HIS3* from Invitrogen *his3-1 leu2-0 met15-0 ura3-0*	WT	a	Invitrogen
JGY1160	BY4741	Pbp1-GFP::*HIS3*, *psk1*::hygro, *psk2*::NAT *his3-1 leu2-0 met15-0 ura3-0*	*psk1psk2*	a	This study
JGY1161	S288C	*psk1*::hygro *psk2*::NAT *ura3-0 trp1-0 SUC2 mal mel gal2 CUP1 flo1 flo8-1*	*psk1psk2*	α	This study

Plasmid	Gene	Description	Backbone	Yeast origin	Selection	Reference or source
pJG9	*PSK1*	Psk1 in pRS424	pRS424	2u	Trp	Jared Rutter
pJG124	EV	EV	pRS424	2u	Trp	Bruce Horazdovsky (Mayo Clinic, Minneapolis, MN)
pJG232	*PSK1*	C-terminal HIS/HA-tagged Psk1	pRS426	2u	Ura	Jared Rutter
pJG410	*PSK1*	Psk1-D1230A in pJG232	pRS426	2u	Ura	DeMille *et al.* (2014)
pJG421	EV	pGAD-C1 empty Y2H prey vector	YEp-GAD	2u	Leu	James *et al.* (1996)
pJG422	EV	pGAD-C2 empty Y2H prey vector	YEp-GAD	2u	Leu	James *et al.* (1996)
pJG423	EV	pGAD-C3 empty Y2H prey vector	YEp-GAD	2u	Leu	James *et al.* (1996)
pJG424	EV	pGBD-C1 empty Y2H bait vector	YEp-GBD	2u	Trp	James *et al.* (1996)
pJG425	EV	pGBD-C2 empty Y2H bait vector	YEp-GBD	2u	Trp	James *et al.* (1996)
pJG441	*PSK1*	Full-length Psk1 in pJG425	YEp-GBD	2u	Trp	DeMille *et al.* (2014)
pJG442	*PSK1*	Full-length Psk1 in pJG422	YEp-GAD	2u	Leu	This study
pJG598	*PSK1*	ΔN692Psk1 in pJG425	YEp-GBD	2u	Trp	DeMille *et al.* (2014)

TABLE 1: Strains, plasmids, and primers used in this study.

Continues

Plasmid	Gene	Description	Backbone	Yeast origin	Selection	Reference or source
pJG709	*PSK1*	ΔN692Psk1 in pJG422	YEp-GAD	2u	Leu	This study
pJG858	*PSK1*	pGAL1-10, Psk1-HIS/HA	pRS426	2u	Ura	DeMille *et al.* (2014)
pJG859	EV	pGAL1-10, HIS/HA	pRS426	2u	Ura	DeMille *et al.* (2014)
pJG925	*PBP1*	Full-length Pbp1 in pJG859	pRS426	2u	Ura	This study
pJG960	*PSK1*	ΔN692Psk1-HIS/HA in pJG858	pRS426	2u	Ura	DeMille *et al.* (2014)
pJG998	EV	pET15b with pGADT7 MCS	pET15b		Amp	This study
pJG1000	*PSK1*	ΔN931Psk1-HIS/HA in pJG858	pRS426	2u	Ura	DeMille *et al.* (2014)
pJG1001	*PBP1*	aa356-722Pbp1	YEp-GAD	2u	Leu	DeMille *et al.* (2014)
pJG1002	*PBP1*	aa197-722Pbp1	YEp-GAD	2u	Leu	DeMille *et al.* (2014)
PJG1003	*PBP1*	aa420-722Pbp1	YEp-GAD	2u	Leu	This study
pJG1004	*PBP1*	aa565-722Pbp1	YEp-GAD	2u	Leu	This study
pJG1008	*PBP1*	Full-length Pbp1	YEp-GAD	2u	Leu	This study
pJG1046	*GAL83*	pGAL1-10, Gal83-HIS/HA	pRS426	2u	Ura	This study
pJG1047	*SIP2*	pGAL1-10, Sip2-HIS/HA	pRS426	2u	Ura	This study
pJG1119	*PSK1*	pGAL1-10, Psk1-RFP	pRS426	2u	Ura	This study
pJG1168	*PBP1*	aa1-565Pbp1	YEp-GAD	2u	Leu	This study
pJG1169	*PBP1*	aa420-565Pbp1	YEp-GAD	2u	Leu	This study
pJG1170	*PSK1*	pGAL1-10-Psk1-D1230A-HIS/HA	pRS426	2u	Ura	DeMille *et al.* (2014)
pJG1181	*PSK1*	pGAL1-10-Psk1-Myc	pRS426	2u	Ura	DeMille *et al.* (2014)
pJG1183	EV	pGAL1-10, EV-Myc	pRS426	2u	Ura	DeMille *et al.* (2014)
pJG1193	*SNF1*	Snf1-8xmyc	pRS313	2u	Ura	Mark Johnston (University of Colorado School of Medicine, Aurora, CO)
pJG1195	*PBP1*	aa470-722Pbp1	YEp-GAD	2u	Leu	This study
pJG1196	*PBP1*	aa1-420Pbp1	YEp-GAD	2u	Leu	This study
pJG1197	*PBP1*	aa1-580Pbp1	YEp-GAD	2u	Leu	This study
pJG1198	*PBP1*	aa1-660Pbp1	YEp-GAD	2u	Leu	This study
pJG1215	*PSK1*	pGAL1-10-Psk1-D1230A-Myc	pRS426	2u	Ura	This study
pJG1216	*PSK1*	pGAL1-10-ΔN931Psk1-Myc	pRS426	2u	Ura	This study
pJG1230	*PBP1*	aa420-580Pbp1	YEp-GAD	2u	Leu	This study
pJG1231	*PBP1*	aa420-660Pbp1	YEp-GAD	2u	Leu	This study
pJG1236	*GAL83*	Gal83 in pJG424	YEp-GBD	2u	Trp	This study
pJG1237	*GAL83*	Gal83 in pJG421	YEp-GAD	2u	Leu	This study
pJG1238	*SIP2*	Sip2 in pJG424	YEp-GBD	2u	Trp	This study
pJG1239	*SIP2*	Sip2 in pJG421	YEp-GAD	2u	Leu	This study
pJG1240	*SNF1*	Snf1 in pJG424	YEp-GBD	2u	Trp	This study
pJG1241	*SNF1*	Snf1 in pJG421	YEp-GAD	2u	Leu	This study
pJG1250	*PBP1*	pGAL1-10, ΔN419Pbp1-Myc	pRS426	2u	Ura	This study
pJG1251	*PBP1*	pGAL1-10, Pbp1-Myc	pRS426	2u	Ura	This study
pJG1258	*GAL83*	aa1-342Gal83 in pJG424	YEp-GBD	2u	Trp	This study
pJG1259	*GAL83*	aa1-342Gal83 in pJG421	YEp-GAD	2u	Leu	This study
pJG1260	*GAL83*	aa141-417Gal83 in pJG424	YEp-GBD	2u	Trp	This study
pJG1261	*GAL83*	aa141-417Gal83 in pJG421	YEp-GAD	2u	Leu	This study

TABLE 1: Strains, plasmids, and primers used in this study.

Continues

Plasmid	Gene	Description	Backbone	Yeast origin	Selection	Reference or source
pJG1262	*GAL83*	aa1-140Gal83 in pJG424	YEp-GBD	2u	Trp	This study
pJG1263	*GAL83*	aa1-140Gal83 in pJG421	YEp-GAD	2u	Leu	This study
pJG1264	*GAL83*	aa141-342Gal83 in pJG424	YEp-GBD	2u	Trp	This study
pJG1265	*GAL83*	aa141-342Gal83 in pJG421	YEp-GAD	2u	Leu	This study
pJG1276	*PSK1*	ΔN931Psk1 in pJG421	YEp-GAD	2u	Leu	This study
pJG1281	*PSK1*	pGAL1-10-ΔN931Psk1-D1230A-Myc	pRS426	2u	Ura	This study
pJG1285	EV	pAdh, EV	pRS414	2u	Trp	Mumberg *et al.* (1995)
pJG1288	SCH9	pAdh-SCH9-HIS	pRS414	2u	Trp	This study

Primer	Sequence
JG1158	TCACCTAACCAACCATTTG
JG2454	GCCCTGCAGTCAAATAACCAACCATTTGTCGTTATTTATG
JG2458	CCGGAATTCGAGGATTTGGCCCACCGAACG
JG2916	GCCTCGAGGTTTATGGCCACTGGTACTACTATTATGG
JG2917	GGCGAATTCATGAAGGGAAACTTTAGGAAAAGAG
JG3136	GGCGAATTCTCGTTGCCTCCAAAACCGATCAGC
JG3137	GGCGAATTCCAACAACGCCAATTGAACTCCATGG
JG3138	GGCGTCGACCTATTTATGGCCACTGGTACTAC
JG3140	CCGGAATTCATGGAGGATTTGGCCCACCGAACG
JG3199	GGCGAATTCATGGCTGGCGACAACCCTGAAAAC
JG3200	GCCGTCGACGTTGCAATGGTGTATACAGTATTTGGGTC
JG3245	GGCGAATTCATGGGTACTACGACAAGTCATCCAG
JG3246	GGCGTCGACGCGAGGACTCTATGGGCGTATAAAG
JG3274	GGCGAATTCATGAGCAGTAACAACAACACAAACAC
JG3275	GCCTCGAGGATTGCTTTGACTGTTAACGGCTAATTCC
JG3330	GGCGAATTCATGATGAATTTTTTTACATC
JG3331	GGCCTCGAGTTAAGCGTAGTCTGGGACGTCGTATGGGTAGCCAGCGTAGTCTGGGACGTCGTATGGGTAGCCAGCG-TAATCCGGAACATCATACGGGTATCCGTGATGATGATGGTGGTGTATTTCGAATCTTCCACTGA
JG3334	GGCCTCGAGTGGCTTCCTCCGAAGACGTTATCAAAG
JG3352	GGCGCATGCTTAGCGATCTACACTAGCACTATCAGCG
JG3384	GGCGAATTCATGTCGTTGCCTCCAAAACCGATCAGC
JG3418	GGCGTCGACGAACCTAGTTTGAGCTTCTTGAATCG
JG3419	GGCGAATTCATGTCGTTGCCTCCAAAACCGATCAGC
JG3432	GGCCATATGATGTTTTCATCATCATCTCGACCTTC
JG3447	GGCGAGCTCCTATGAGCGATCCCGTTTTGTGAAC
JG3460	GGCGAATTCACTTCATTGAGAAGACGTAATCATGGTTCC
JG3461	GGCGTCGACCGAAGAATTAGATTTTAATGTAGAGCTTG
JG3462	GGCGTCGACAGCTTCTTGAATCGCCGTATCCTCATC
JG3463	GGCGTCGACGCTACCCATAACTGGCATCATTTGAGGC
JG3530	GGCGTCGACGGCCTTGATTTTGAAGTGAGTCAGGC
JG3531	GGCGAATTCTTTCAACAGCAACAAGAACAGCAACAG
JG3532	GGCGTCGACGGGCCATATTTTGGTGATTATTTTGCTGC
JG3533	GGCGAATTCTGGTTGACTCCTCCACAACTGCC

TABLE 1: Strains, plasmids, and primers used in this study. Continued

1 mM β-mercaptoethanol, cOmplete Protease Inhibitor Cocktail Tablet, pH 7.4, with phosphatase inhibitors when necessary). Resuspended cultures were lysed using the Microfluidics M-110P homogenizer (Microfluidics, Westwood, MA [for 500-ml cultures]) or bead blasted for 1 min, followed by 1 min on ice repeated three times using 0.2-mm glass beads (for 100-ml cultures). Cell debris was then pelleted at 12,000 rpm for 20–30 min. Supernates were transferred to new tubes and incubated with 200 µl of nickel-nitrilotriacetic acid (Ni-NTA) agarose beads (Qiagen, Valencia, CA [for 500-ml HIS purification]) or 5–10 µl of Myc-conjugated magnetic beads (Cell Signaling, Danvers, MA [for 100-ml Myc purification]) for 2–3 h at 4°C. For HIS-epitope purification, beads were washed twice with 15 ml of lysis buffer and then transferred to a polypropylene column and washed with 30–50 ml of lysis buffer. For Myc-protein purification, beads were separated using magnetic force and washed four times with 500 µl of lysis buffer lacking the protease inhibitor. HIS-tagged proteins were eluted three times with 0.3 ml of lysis buffer containing 250 mM imidazole and 100 mM NaCl but lacking protease and phosphatase inhibitors. Beads containing Myc-tagged proteins were used directly for in vitro kinase assays without eluting.

Quantification of in vivo phosphorylation of Ugp1

As a measure of Psk1 activity, the amount of Ugp1 phosphorylated in vivo was assessed. Briefly, an overnight sample of Psk2-deficient cells (*PSK1psk2,* JGY3) was diluted 1:100 in yeast extract/peptone/dextrose/adenine (YPAD) and grown for 3–4 h at 30°C to an OD_{600} of 0.5. Medium was then changed by filtering with a 0.2-µm filter and resuspending in YPA-raffinose (2%). Cells were harvested at various time points by filtering and flash freezing at –80°C. Percentage Ugp1 phosphorylated was assayed as previously described (Smith and Rutter, 2007). Briefly, cells were lysed by bead blast, and the supernatant was fractionated on a monoQ column, which separates the phosphorylated and unphosphorylated forms of Ugp1. The activity of Ugp1 in each fraction was assessed, and the percentage of phosphorylated Ugp1 was calculated by fitting the sum of two Gaussians to the curves to determine the area under the peak using KaleidaGraph (Synergy Software, Reading, PA).

In vivo Psk1 EMSA

HIS-HA epitope-tagged Psk1 (pJG858) was purified from WT (JGY1), *snf1* (JGY91), and *reg1* (JGY95) yeast grown in galactose, run on 8% SDS–PAGE, and silver stained to visualize any electrophoretic mobility shift.

In vitro kinase assays

Constructs of Psk1-Myc and Pbp1-Myc epitope-tagged plasmids were made as follows: full-length Pbp1 (pJG1251) was constructed by PCR amplification using primers JG2916/2917 and cloning into the *Eco*RI/*Xho*I sites of pJG1183. ΔN419Pbp1 (pJG1250) was constructed by PCR amplification using primers JG3384/2916 and cloning into the *Eco*RI/*Xho*I sites of pJG1183. ΔN931Psk1 (pJG1216) was constructed by PCR amplification using primers JG3140/1158 and cloning into the *Eco*RI/*Xho*I sites of pJG1181. Full-length Psk1-D1230A (kinase dead) (pJG1215) was constructed by digesting pJG410 and subcloning into *Bgl*II/*Xho*I sites of pJG1181. ΔN931Psk1-D1230A (pJG1281) was constructed by PCR amplification of pJG1170 using primers JG3140/1158 and cloning into the *Eco*RI/*Xho*I sites of pJG1181. Full-length Psk1 (pJG1181) was made previously (DeMille *et al.*, 2014).

Full-length Psk1 and ΔN931Psk1 were purified from WT yeast (JGY1), and kinase-dead Psk1 and both Pbp1 constructs were purified from *psk1psk2* yeast (JGY4). Purified full-length and ΔN419Pbp1-Myc–tagged proteins were assayed for PAS kinase–dependent phosphorylation by incubating purified protein in 30 µl of reaction buffer containing 1× Psk1 kinase buffer (0.4 M HEPES, 0.1 M KCl, 5 mM $MgCl_2$, pH 7.0), 0.2 mM ATP, ^{32}P-ATP [5 µCi; MP Biomedicals, Santa Ana, CA]) in the presence or absence of purified full-length Psk1, truncated ΔN931Psk1, or kinase-dead Psk1-D1230A. Kinase assays were started with the addition of Psk1 and stopped with SDS–PAGE sample buffer. Reactions were incubated for 12 min at 30°C. For in vitro kinase assays of Snf1 (pJG1193) and Psk1-D1230A (pJG1215) or ΔN931Psk1-D1230A (pJG1281), reaction conditions were similar, except the following changes: 1× Snf1 kinase buffer (50 mM Tris-HCl, 10 mM $MgCl_2$, 1 mM dithiothreitol [DTT], pH 7.5), 10 µM ATP, and 7.5 µCi of ^{32}P-ATP, and reactions were incubated for 35 min.

In vivo Pbp1 phosphostate analysis

Pbp1-HIS expressed under the GAL1-10 promoter (pJG925) was made by PCR amplifying Pbp1 with primers JG2916/2917 and cloning into the *Eco*RI/*Xho*I sites of pJG859. HIS-tagged Pbp1 (pJG925) was expressed in JGY1 (WT) overexpressing full-length Psk1 on a plasmid (pJG9) or in JGY4 (*psk1psk2*) containing an empty vector (pJG124). Proteins were grown in duplicate in SD-Ura overnight, induced with SGal-Ura for 36 h, and purified on Ni-NTA as described. Eluates were run on 8% SDS–PAGE, transferred to nitrocellulose membrane, and incubated overnight with nonspecific Phospho-Threonine (Cell Signaling Technology) antibody. Blots were imaged, stripped, and then incubated overnight with PhosphoSerine (Q5; Qiagen) antibody. Total Pbp1 was assessed by stripping the membrane once more, incubating overnight with hemagglutinin (HA) antibody (Roche), and imaging.

Microscopy

Pbp1-GFP fusion yeast (JGY1144) was obtained from the Invitrogen yeast-GFP clone collection (Invitrogen, Grand Island, NY) and transformed with Psk1-RFP (pJG1119) for colocalization analysis. pJG1119 was made by PCR amplification of dsRED using JG3334/3352 and BBa_J04450 (iGEM registry plasmid) as DNA template and cloned into the *Xho*I/*Sph*I sites of pJG858 to replace the HISHA tag with the RFP fusion. Overnight samples were grown in SD-Ura medium, and then yeast were pelleted and resuspended in SGal-Ura medium to induce expression of Psk1-RFP. Cultures were grown in SGal-Ura for 3–5 d, cells were pelleted, washed once with synthetic complete (SC) medium lacking a carbon source, and resuspended in fresh SC medium. Cultures were incubated at 30°C for an additional 1 h to allow them to grow under glucose deprivation conditions. Images were then captured using a FluoView FV1000 confocal laser-scanning microscope (Olympus, Tokyo, Japan) with 60× magnification lens and the appropriate filter sets (GFP, dsRED). For percentage of Pbp1-GFP foci in WT (JGY1144) and *psk1psk2* (JGY1160) yeast, strains were grown in SD complete medium for 4 d and then washed, resuspended in SC lacking a carbon source, incubated, and imaged as described. For percentage of Psk1 and Pbp1 colocalization, 50 cells (96 distinct cytoplasmic foci) were counted. For percentage of Pbp1-GFP foci, 1199 cells for WT and 782 for *psk1psk2* were counted. SEM was used for error bars, and Student's *t* test was used for statistical significance calculations.

Sch9 phosphorylation assays

A plasmid expressing Sch9 under the ADH1 promoter (pJG1288) was made by amplifying Sch9-HIS using primers JG3330 and JG3331

and cloning into pJG1285. This Sch9 plasmid was transformed into yeast (WT [JGY1], *reg1* [JGY95], *snf1* [JGY91], *reg1psk1psk2* [JGY283], *reg1snf1psk1psk2* [JGY280]), grown in SD-Trp overnight, and then diluted 1:100 into YPAD and grown until OD_{600} ~1.0. For rapamycin controls, 100 nM rapamycin (Research Products International, Mount Prospect, IL) was added 1 h before harvesting cells. Preparation of Sch9 protein extract was performed as described by Miller-Fleming *et al*. (2014). Samples were normalized and loaded on 8% SDS–PAGE, transferred to nitrocellulose membrane, and incubated overnight with anti–phospho-Thr737-Sch9 and anti–Thr737-Sch9 antibodies (Kingsbury *et al.*, 2014). Intensity signals were quantified using ImageJ (National Institutes of Health, Bethesda, MD).

Mass spectrometry

Psk1 samples were prepared using a modified version of filter-aided sample preparation (Wisniewski *et al.*, 2009). Briefly, samples were placed on filters, denatured by adding 8 M urea (Molecular Biology Grade; EMD Chemicals, Gibbstown, NJ), reduced with dithiothreitol (DTT, Sigma-Aldrich), alkylated with iodoacetamide (BioUltra Grade; Sigma-Aldrich), and digested with trypsin (Sequencing Grade Modified; Promega, Madison, WI). Digested protein was analyzed by LC-MS using the Eksigent NanoLC Ultra coupled with the LTQ Orbitrap XL mass spectrometer. Peptides were separated on a Waters Peptide Separation Technology c18 column with a water/acetonitrile gradient containing 0.1% formic acid (Optima LC-MS Grade, Fisher Scientific, Pittsburgh, PA). MS scans were collected in the Orbitrap. Fragmentation scans were collected in the LTQ, excluding charge state 1 and unassigned charge states using collision [induced dissociation (CID). MS^2 multistage activation or MS^3 CID (Kall *et al.*, 2007) was used, with neutral losses corresponding to phosphate groups (32.66, 48.99, and 97.97 *m/z*) in some cases (Schroeder *et al.*, 2004).

Data were analyzed using Mascot, Sequest, and/or Sequest HT with or without Percolator (Perkins *et al.*, 1999; Tabb *et al.*, 2001; Kall *et al.*, 2007). The Proteome Discoverer Package was also used on some samples. Search settings included dynamic modifications: phosphorylation (STY) and oxidation (M). Carbamidomethyl (C) was set as a dynamic or static modification. Searches were performed against the uni_yeast database or a modified uni_yeast database containing 6× HIS-tagged Psk1 (UniProt, 2014).

ACKNOWLEDGMENTS

We thank Mark Johnston (University of Colorado School of Medicine, Aurora, CO) for the generous gift of a functional Snf1-Myc construct and Maria Cardenas (Duke University, Durham, NC) for the generous gift of anti–phospho-Thr737-Sch9 and anti–Thr737-Sch9 antibodies. We also thank John T. Prince (Brigham Young University, Provo, UT) for aid with the mass spectrometry experiments. This work was supported by National Institutes of Health Grant R15 GM100376-01, a Brigham Young University Mentoring Environmental Grant to J.H.G., Brigham Young University Cancer Research Center Fellowships to B.D.B. and J.F.A., and the Brigham Young University Department of Microbiology and Molecular Biology and College of Life Sciences.

REFERENCES

Amezcua CA, Harper SM, Rutter J, Gardner KH (2002). Structure and interactions of PAS kinase N-terminal PAS domain: model for intramolecular kinase regulation. Structure 10, 1349–1361.

An R, da Silva Xavier G, Hao HX, Semplici F, Rutter J, Rutter GA (2006). Regulation by Per-Arnt-Sim (PAS) kinase of pancreatic duodenal homeobox-1 nuclear import in pancreatic beta-cells. Biochem Soc Trans 34, 791–793.

Bolster DR, Crozier SJ, Kimball SR, Jefferson LS (2002). AMP-activated protein kinase suppresses protein synthesis in rat skeletal muscle through down-regulated mammalian target of rapamycin (mTOR) signaling. J Biol Chem 277, 23977–23980.

Borza LR (2014). A review on the cause-effect relationship between oxidative stress and toxic proteins in the pathogenesis of neurodegenerative diseases. Rev Med Chir Soc Med Nat Iasi 118, 19–27.

Broach JR (2012). Nutritional control of growth and development in yeast. Genetics 192, 73–105.

Burkewitz K, Zhang Y, Mair WB (2014). AMPK at the nexus of energetics and aging. Cell Metab 20, 10–25.

Cardon CM, Beck T, Hall MN, Rutter J (2012). PAS kinase promotes cell survival and growth through activation of Rho1. Sci Signal 5, ra9.

Cardon CM, Rutter J (2012). PAS kinase: integrating nutrient sensing with nutrient partitioning. Semin Cell Dev Biol 23, 626–630.

Cheng SW, Fryer LG, Carling D, Shepherd PR (2004). Thr2446 is a novel mammalian target of rapamycin (mTOR) phosphorylation site regulated by nutrient status. J Biol Chem 279, 15719–15722.

da Silva Xavier G, Farhan H, Kim H, Caxaria S, Johnson P, Hughes S, Bugliani M, Marselli L, Marchetti P, Birzele F, *et al.* (2011). Per-arnt-sim (PAS) domain-containing protein kinase is downregulated in human islets in type 2 diabetes and regulates glucagon secretion. Diabetologia 54, 819–827.

da Silva Xavier G, Rutter J, Rutter GA (2004). Involvement of Per-Arnt-Sim (PAS) kinase in the stimulation of preproinsulin and pancreatic duodenum homeobox 1 gene expression by glucose. Proc Natl Acad Sci USA 101, 8319–8324.

DeMille D, Bikman BT, Mathis AD, Prince JT, Mackay JT, Sowa SW, Hall TD, Grose JH (2014). A comprehensive protein-protein interactome for yeast PAS Kinase 1 Reveals direct inhibition of respiration through the phosphorylation of Cbf1. Mol Biol Cell 25, 2199–2215.

Eglen R, Reisine T (2011). Drug discovery and the human kinome: recent trends. Pharmacol Ther 130, 144–156.

Fang Z, Grutter C, Rauh D (2013). Strategies for the selective regulation of kinases with allosteric modulators: exploiting exclusive structural features. ACS Chem Biol 8, 58–70.

Ghillebert R, Swinnen E, Wen J, Vandesteene L, Ramon M, Norga K, Rolland F, Winderickx J (2011). The AMPK/SNF1/SnRK1 fuel gauge and energy regulator: structure, function and regulation. FEBS J 278, 3978–3990.

Grose JH, Smith TL, Sabic H, Rutter J (2007). Yeast PAS kinase coordinates glucose partitioning in response to metabolic and cell integrity signaling. EMBO J 26, 4824–4830.

Grose JH, Sundwall E, Rutter J (2009). Regulation and function of yeast PAS kinase: a role in the maintenance of cellular integrity. Cell Cycle 8, 1824–1832.

Hao HX, Cardon CM, Swiatek W, Cooksey RC, Smith TL, Wilde J, Boudina S, Abel ED, McClain DA, Rutter J (2007). PAS kinase is required for normal cellular energy balance. Proc Natl Acad Sci USA 104, 15466–15471.

Hardie DG (2013). AMPK: a target for drugs and natural products with effects on both diabetes and cancer. Diabetes 62, 2164–2172.

Hughes Hallett JE, Luo X, Capaldi AP (2014). State transitions in the TORC1 signaling pathway and information processing in Saccharomyces cerevisiae. Genetics 198, 773–786.

Hurtado-Carneiro V, Roncero I, Blazquez E, Alvarez E, Sanz C (2013). PAS kinase as a nutrient sensor in neuroblastoma and hypothalamic cells required for the normal expression and activity of other cellular nutrient and energy sensors. Mol Neurobiol 48, 904–920.

Hurtado-Carneiro V, Roncero I, Egger SS, Wenger RH, Blazquez E, Sanz C, Alvarez E (2014). PAS kinase is a nutrient and energy sensor in hypothalamic areas required for the normal function of AMPK and mTOR/S6K1. Mol Neurobiol 50, 314–326.

Inoki K, Li Y, Xu T, Guan KL (2003a). Rheb GTPase is a direct target of TSC2 GAP activity and regulates mTOR signaling. Genes Dev 17, 1829–1834.

Inoki K, Ouyang H, Zhu T, Lindvall C, Wang Y, Zhang X, Yang Q, Bennett C, Harada Y, Stankunas K, *et al.* (2006). TSC2 integrates Wnt and energy signals via a coordinated phosphorylation by AMPK and GSK3 to regulate cell growth. Cell 126, 955–968.

Inoki K, Zhu T, Guan KL (2003b). TSC2 mediates cellular energy response to control cell growth and survival. Cell 115, 577–590.

James P, Halladay J, Craig EA (1996). Genomic libraries and a host strain designed for highly efficient two-hybrid selection in yeast. Genetics 144, 1425–1436.

Jiang R, Carlson M (1997). The Snf1 protein kinase and its activating subunit, Snf4, interact with distinct domains of the Sip1/Sip2/Gal83 component in the kinase complex. Mol Cell Biol 17, 2099–2106.

Kaehler C, Isensee J, Nonhoff U, Terrey M, Hucho T, Lehrach H, Krobitsch S (2012). Ataxin-2-like is a regulator of stress granules and processing bodies. PLoS One 7, e50134.
Kall L, Canterbury JD, Weston J, Noble WS, MacCoss MJ (2007). Semi-supervised learning for peptide identification from shotgun proteomics datasets. Nat Methods 4, 923–925.
Khan KH, Yap TA, Yan L, Cunningham D (2013). Targeting the PI3K-AKT-mTOR signaling network in cancer. Chin J Cancer 32, 253–265.
Kimura Y, Irie K, Irie K (2013). Pbp1 is involved in Ccr4- and Khd1-mediated regulation of cell growth through association with ribosomal proteins Rpl12a and Rpl12b. Eukaryot Cell 12, 864–874.
Kimura N, Tokunaga C, Dalal S, Richardson C, Yoshino K, Hara K, Kemp BE, Witters LA, Mimura O, Yonezawa K (2003). A possible linkage between AMP-activated protein kinase (AMPK) and mammalian target of rapamycin (mTOR) signalling pathway. Genes Cells 8, 65–79.
Kingsbury JM, Sen ND, Maeda T, Heitman J, Cardenas ME (2014). Endo-lysosomal membrane trafficking complexes drive nutrient-dependent TORC1 signaling to control cell growth in Saccharomyces cerevisiae. Genetics 196, 1077–1089.
Lal H, Kolaja KL, Force T (2013). Cancer genetics and the cardiotoxicity of the therapeutics. J Am Coll Cardiol 61, 267–274.
Laplante M, Sabatini DM (2012). mTOR signaling in growth control and disease. Cell 149, 274–293.
Liu WY, Jiang RS (2013). Advances in the research of AMPK and its subunit genes. Pak J Biol Sci 16, 1459–1468.
Loewith R, Hall MN (2011). Target of rapamycin (TOR) in nutrient signaling and growth control. Genetics 189, 1177–1201.
Ludin K, Jiang R, Carlson M (1998). Glucose-regulated interaction of a regulatory subunit of protein phosphatase 1 with the Snf1 protein kinase in Saccharomyces cerevisiae. Proc Natl Acad Sci USA 95, 6245–6250.
Magana JJ, Velazquez-Perez L, Cisneros B (2013). Spinocerebellar ataxia type 2: clinical presentation, molecular mechanisms, and therapeutic perspectives. Mol Neurobiol 47, 90–104.
Mangus DA, Amrani N, Jacobson A (1998). Pbp1p, a factor interacting with Saccharomyces cerevisiae poly(A)-binding protein, regulates polyadenylation. Mol Cell Biol 18, 7383–7396.
Mangus DA, Smith MM, McSweeney JM, Jacobson A (2004). Identification of factors regulating poly(A) tail synthesis and maturation. Mol Cell Biol 24, 4196–4206.
Miller-Fleming L, Cheong H, Antas P, Klionsky DJ (2014). Detection of Saccharomyces cerevisiae Atg13 by western blot. Autophagy 10, 514–517.
Momcilovic M, Iram SH, Liu Y, Carlson M (2008). Roles of the glycogen-binding domain and Snf4 in glucose inhibition of SNF1 protein kinase. J Biol Chem 283, 19521–19529.
Mumberg D, Muller R, Funk M (1995). Yeast vectors for the controlled expression of heterologous proteins in different genetic backgrounds. Gene 156, 119–122.
Nonhoff U, Ralser M, Welzel F, Piccini I, Balzereit D, Yaspo ML, Lehrach H, Krobitsch S (2007). Ataxin-2 interacts with the DEAD/H-box RNA helicase DDX6 and interferes with P-bodies and stress granules. Mol Biol Cell 18, 1385–1396.
Perkins DN, Pappin DJ, Creasy DM, Cottrell JS (1999). Probability-based protein identification by searching sequence databases using mass spectrometry data. Electrophoresis 20, 3551–3567.
Porta C, Paglino C, Mosca A (2014). Targeting PI3K/Akt/mTOR signaling in cancer. Front Oncol 4, 64.
Quinn BJ, Kitagawa H, Memmott RM, Gills JJ, Dennis PA (2013). Repositioning metformin for cancer prevention and treatment. Trends Endocrinol Metab 24, 469–480.
Reiter AK, Bolster DR, Crozier SJ, Kimball SR, Jefferson LS (2005). Repression of protein synthesis and mTOR signaling in rat liver mediated by the AMPK activator aminoimidazole carboxamide ribonucleoside. Am J Physiol Endocrinol Metab 288, E980–E988.
Rosilio C, Ben-Sahra I, Bost F, Peyron JF (2014). Metformin: a metabolic disruptor and anti-diabetic drug to target human leukemia. Cancer Lett 346, 188–196.
Rutter J, Michnoff CH, Harper SM, Gardner KH, McKnight SL (2001). PAS kinase: an evolutionarily conserved PAS domain-regulated serine/threonine kinase. Proc Natl Acad Sci USA 98, 8991–8996.
Rutter J, Probst BL, McKnight SL (2002). Coordinate regulation of sugar flux and translation by PAS kinase. Cell 111, 17–28.
Schmidt MC, McCartney RR (2000). beta-subunits of Snf1 kinase are required for kinase function and substrate definition. EMBO J 19, 4936–4943.
Schroeder MJ, Shabanowitz J, Schwartz JC, Hunt DF, Coon JJ (2004). A neutral loss activation method for improved phosphopeptide sequence analysis by quadrupole ion trap mass spectrometry. Anal Chem 76, 3590–3598.
Semache M, Fontes G, Fogarty S, Kikani C, Rutter J, Poitout V (2013). PAS kinase regulates PDX-1 protein stability via phosphorylation of GSK-3beta in pancreatic beta cells. Can J Diabetes 37(Suppl 4), S59.
Semplici F, Vaxillaire M, Fogarty S, Semache M, Bonnefond A, Fontes G, Philippe J, Meur G, Diraison F, Sessions RB, *et al.* (2011). Human mutation within Per-Arnt-Sim (PAS) domain-containing protein kinase (PASK) causes basal insulin hypersecretion. J Biol Chem 286, 44005–44014.
Shimobayashi M, Hall MN (2014). Making new contacts: the mTOR network in metabolism and signalling crosstalk. Nat Rev Mol Cell Biol 15, 155–162.
Smith TL, Rutter J (2007). Regulation of glucose partitioning by PAS kinase and Ugp1 phosphorylation. Mol Cell 26, 491–499.
Swisher KD, Parker R (2010). Localization to, and effects of Pbp1, Pbp4, Lsm12, Dhh1, and Pab1 on stress granules in Saccharomyces cerevisiae. PLoS One 5, e10006.
Tabb DL, Eng JK, Yates JRIII (2001). Protein identification by SEQUEST. In: Proteome Research: Mass Spectrometry, Vol 1, ed. P James, Berlin: Springer-Verlag, 125–142.
Takahara T, Maeda T (2012). Transient sequestration of TORC1 into stress granules during heat stress. Mol Cell 47, 242–252.
UniProt C (2014). Activities at the Universal Protein Resource (UniProt). Nucleic Acids Res 42, D191–D198.
Urban J, Soulard A, Huber A, Lippman S, Mukhopadhyay D, Deloche O, Wanke V, Anrather D, Ammerer G, Riezman H, *et al.* (2007). Sch9 is a major target of TORC1 in Saccharomyces cerevisiae. Mol Cell 26, 663–674.
Vincent O, Carlson M (1999). Gal83 mediates the interaction of the Snf1 kinase complex with the transcription activator Sip4. EMBO J 18, 6672–6681.
Wilson WA, Skurat AV, Probst B, de Paoli-Roach A, Roach PJ, Rutter J (2005). Control of mammalian glycogen synthase by PAS kinase. Proc Natl Acad Sci USA 102, 16596–16601.
Wisniewski JR, Zougman A, Nagaraj N, Mann M (2009). Universal sample preparation method for proteome analysis. Nat Methods 6, 359–362.
Wu X, Romero D, Swiatek WI, Dorweiler I, Kikani CK, Sabic H, Zweifel BS, McKearn J, Blitzer JT, Nickols GA, *et al.* (2014). PAS kinase drives lipogenesis through SREBP-1 maturation. Cell Rep 8, 242–255.
Ye T, Bendrioua L, Carmena D, Garcia-Salcedo R, Dahl P, Carling D, Hohmann S (2014). The mammalian AMP-activated protein kinase complex mediates glucose regulation of gene expression in the yeast Saccharomyces cerevisiae. FEBS Lett 588, 2070–2077.
Zhang L, Daly RJ (2012). Targeting the human kinome for cancer therapy: current perspectives. Crit Rev Oncog 17, 233–246.